ORIGINAL RESEARCH

Global Dynamics in a Beddington–DeAngelis Prey–Predator Model with Density Dependent Death Rate of Predator

Koushik Garain[1] · Udai Kumar[1] · Partha Sarathi Mandal[1]

Abstract

The article aims to investigate a prey–predator model which includes density dependent death rate for predators and Beddington–DeAangelis type functional response. We observe the changes in the existence and stability of the equilibrium points and investigate the complete global dynamics of the model. A two-parametric bifurcation diagram has been described here which shows the effect of density dependent death rate parameter of predator. We have also examined all possible local and global bifurcations that the system could go through, namely transcritical bifurcation, saddle-node bifurcation, Hopf-bifurcation, cusp bifurcation, Bogdanov–Takens bifurcation, Bautin bifurcation and homoclinic bifurcation.

Keywords Predator–prey model · Beddington–DeAngelis · Functional response · Stability analysis · Bifurcation · Global dynamics

Introduction

After developing by Lotka [23] and Volterra [39], several researchers observed the dynamical analysis of ecological systems, modeled with ordinary differential equations. Lotka and Volterra first introduced the classical prey–predator intersection model and based upon this various two dimensional models are analyzed to understand the nature of intersection within prey and predator species. For a prey–predator model it is important to choose a proper functional response. Functional response is the interaction between predator-prey species and it refers how much a single predator consumed prey population density per unit time. In 1965, after several experiments, Holling [16] suggested three different types of functional responses like Holling type I, Holling type II and Holling type III to model the phenomena of predation. Depend on these functional responses, several researchers have investigated a large variety of dynamical systems ranging from simple two dimensional models to higher dimensional models to understand the nature of intersection between prey and predator species within the deterministic environment [12–14,16].

Holling type I (or Lotka–Volterra) functional response is one-dimensional and it is the simple form of functional response as intake rate is constant here. But, the more reasonable

✉ Partha Sarathi Mandal
   parthas@nitp.ac.in

[1] Department of Mathematics, NIT Patna, Patna, Bihar 800005, India

functional response will be nonlinear. For Holling type II functional response, when prey population density is high, the predator grows at a maximum relative growth rate α, whereas at low prey densities Φ approximates the LotkaVolterra model (as $\Phi \to \frac{\alpha x}{m}$ when prey density x is at very low level), where $\Phi(x(t))$ is the functional response. On the other hand, for Holling type III functional response, growth curve becomes quadratic instead of linear at low prey population densities ($\Phi \to \frac{\alpha x^2}{m}$ when prey density x is at very low level). The prey–predator model with Holling-type functional response are strictly prey-dependent. Since 1959, Holling's prey dependent type II functional response was the key on prey–predator theory [34]. The Beddington–DeAngelis functional response which is introduced by Beddington [5] and DeAngelis [10] is similar to the Holling type II functional response but an extra term in the denominator which is depend upon predator. The ratio-dependent functional response also incorporates mutual interference by predators, but at low densities it has singular behaviour. For mathematical analysis [19] and the references in [9] for some debate among biologists about ratio dependence. For different mathematical representations of the functional response, readers are referred to [3,8,13,16,18,27]. The Beddington–DeAngelis functional response has some similar qualitative features as the ratio-dependent form but at low densities it keeps away from some of the behaviors of it. It is known that Beddington–DeAngelis type functional response is most acceptable than other available response functions and it has the ability to take care of a number of ecological mechanisms [5,9]. This type of functional response not only describe that two or more predator encounters prey but also explain that predators spend some time to encounters other predator also. When predator density is very high then feeding rate of predator decreases due to mutual interference among the predators and in this case Holling type functional response is not appropriate. This is the reason for the modification of Holling type II functional response in the form of BeddingtonDeAngelis functional response. Several mathematical models including the Beddington–DeAngelis type functional response have been investigated [6,11,21,22,35–38] and it also produce very rich and biologically reasonable dynamics . In [6], Cantrell and Cosner have studied a prey–predator model with Beddington–DeAngelis functional response and they analysed various dynamical properties like stability, limit cycle, etc. In 2005, Dimitrov and Kojouharov [11] considered a predator–prey model with Beddington–DeAngelis functional response and linear intrinsic growth rate of the prey population and shown that mutual interference between predators can alone stabilize predator–prey interactions even when only a linear intrinsic growth rate of the prey population is considered in the mathematical model. In this model density dependent death rate of predator was not considered. In [22], Liu and Wang have studied the global stability of the prey–predator model with Beddington–DeAngelis functional response. In 2018, Tripathi et.al. [35] investigated the role of reserved region and degree of mutual interference among predators in the dynamics of system and obtained different conditions that affect the persistence of the system.

In a prey–predator model density dependent death rate of predator has significant amount of effect on the system. There are very few researchers analyzed the fact that include the role of density dependent death rate of predators to the system dynamics [2,28,30]. Inspired by the above facts, in this paper we consider a prey–predator model with the Beddington–DeAngelis functional response and density dependent death rate of predator. Hence, it is very important to know the significant effect of the Beddington–DeAngelis functional response and density dependent death rate of predator on the system and to the best of our knowledge this model along with global dynamics has yet not been investigated by any one. Clearly, our model is the generalization of the model [6,11,21,22]. In this work, we show that the conversion rate of prey and density dependent death rate of predator have an important role

in the dynamics of the system. We show that the stable coexisting steady-state is possible when density dependent death rate is very high. Complete stability analysis of the system and global dynamics of the system are presented to investigate the influence of conversion rate parameter and density dependent death rate parameter. We find that, oscillatory coexistence of both the prey and predator populations is possible for low intraspecific competition rate of predator. When consumption rate is low, coexistence state of both the species occur through transcritical bifurcation and when consumption rate is high, more than one equilibrium state of both the species is observed for low intraspecific competition rate of predator. We also compare the dynamics of the system with [11].

The present paper is represented as follows: in "Development of the Model" section, we discuss the basic model with dimensionless variables and parameters. We also check that the solution is always bounded and positive in this section. In "Stability of Equilibria and Local Bifurcation" section, we discuss the existence and stability of the equilibrium points. Also we study several local bifurcations, namely, transcritical bifurcation, saddle-node bifurcation, Hopf-bifurcation; which are of codimension one and the system also undergoes different types of codimension two bifurcations, namely, cusp bifurcation, Bogdanov–Takens bifurcation and Bautin bifurcation in this section. In "Global Dynamics" section, we discuss the global dynamics of the system. In this section, comparison between the dynamics of our system with [11] is also given. Ecological interpretations of obtained results are provided in "Discussion" section.

Development of the Model

First classical prey–predator interaction model proposed by Lotka and Volterra is given by the following system of equations [23,39]:

$$\frac{dx}{dt} = xf(x) - g(x, y)y,$$
$$\frac{dy}{dt} = pg(x, y)y - dy,$$

where $x(t)$ and $y(t)$ denote the prey and predator density at time t respectively. $f(x)$ is the prey growth rate in the absence of predator and $g(x, y)$ is the predator's functional response. Parameters p and d stand for conversion rate of prey and death rate of predator, respectively. Here, we consider the logistic functional response in the prey growth equation, and hence the expression of $f(x)$ is given by

$$f(x) = rx\left(1 - \frac{x}{k}\right),$$

where r is the prey intrinsic growth rate and k is environmental carrying capacity for prey. Also, we consider the functional response of predator to be Beddington–DeAngelis type and it is given by

$$g(x, y) = \frac{cxy}{a + x + by},$$

where c represents consumption rate, a is the saturation constant and b is predator interference rate. We also add density dependent death rate for the predator. In the present work, we consider the following prey–predator model with logistic functional response in the prey growth, Beddington–DeAngelis functional response and density dependent death rate for the

predator. The prey–predator model is represented by the following two nonlinear ordinary differential equations,

$$\frac{dx}{dt} = rx\left(1 - \frac{x}{k}\right) - \frac{cxy}{a + x + by}, \tag{1}$$

$$\frac{dy}{dt} = \frac{pcxy}{a + x + by} - \gamma y - \delta y^2, \tag{2}$$

where δ is the predator intraspecific competition rate and initial conditions should be non negative, i.e $x(0) \geq 0$, $y(0) \geq 0$. All parameters are positive constants. To reduce the number of parameters, we use the following model with dimensionless variables defined by $x = ku$, $y = kv$ and $t = \frac{T}{r}$,

$$\frac{du}{dT} = u(1 - u) - \frac{\alpha u v}{A + u + Bv}, \tag{3}$$

$$\frac{dv}{dT} = \frac{Suv}{A + u + Bv} - Qv - Rv^2, \tag{4}$$

where $\alpha = \frac{c}{r}$, $A = \frac{a}{k}$, $B = b$, $S = \frac{pc}{r}$, $Q = \frac{\gamma}{r}$, $R = \frac{\delta k}{r}$ are dimensionless parameters.

Positivity of Solution

From Eqs. (3)–(4), we can write,

$$u(T) = u(0)exp\left[\int_0^T \left((1 - u(s)) - \frac{\alpha v(s)}{A + u(s) + Bv(s)}\right)ds\right],$$

$$v(T) = v(0)exp\left[\int_0^T \left(\frac{Su(s)}{A + u(s) + Bv(s)} - Q - R(s)\right)ds\right].$$

From above it is clear that $u(T) > 0$ and $v(T) > 0$ whenever $u(0) > 0$, $v(0) > 0$. Hence any solution from first quadrant of uv-plane gives always a positive solution. Further we can verify that any solution trajectories starting from $(u, 0)$ with $u > 0$, remain within the positive u-axis and same result follows for positive v-axis. Hence, the set $(u, v) : u, v \geq 0$ is an invariant set.

Boundedness of Solution

In order to prove the boundedness of the solution we have to consider two cases $0 < u(0) < 1$ and $u(0) > 1$. From Eq. (3), we can write,

$$u(T) = u(0)exp\left[\int_0^T N(u(s), v(s))ds\right],$$

where $N(u(s), v(s)) = \left((1 - u(s)) - \frac{\alpha v(s)}{A+u(s)+Bv(s)}\right)$. Now

Case I: Consider $0 < u(0) < 1$, our clam is $u(T) \leq 1$ otherwise there exist two real number T_1 and T_2 with $T_2 > T_1$ such that $u(T_1) = 1$ and $u(T) > 1$ for $T \in (T_1, T_2)$. Then,

$$u(T) = u(0)exp\left[\int_0^T N(u(s), v(s))ds\right]$$

$$= u(0)exp\left[\int_0^{T_1} N(u(s), v(s))ds\right]exp\left[\int_{T_1}^T N(u(s), v(s))ds\right]$$

$$(since, e^{x+y} = e^x * e^y \ if \ xy = yx)$$

$$= u(T_1)exp\left[\int_{T_1}^T N(u(s), v(s))ds\right] < u(T_1),$$

as $N(u(s), v(s)) < 0 \ \forall \ T \in (T_1, T_2)$, Which contradict our hypothesis. So $u(T) \le 1$ for all $T > 0$.

Case II: Now consider $u(0) > 1$ so $u(T) > 1$ also, Then,

$$u(T) = u(0)exp\left[\int_0^T N(u(s), v(s))ds\right] < u(0),$$

as $N(u(s), v(s)) < 0$ for $u(T) > 1$.

Hence from the both cases we can say that any positive solution satisfy $u(T) \le max[u(0), 1]$ for all $T > 0$.

Again from (4), we have

$$\limsup_{T \to \infty} v(T) \le \frac{S - Q}{R}.$$

Parametric restriction should be $S > Q$ as population densities are always positive.

Stability of Equilibria and Local Bifurcation

In this section we examine the possible number of equilibria of the system and their stability followed by the details bifurcation analysis of the system.
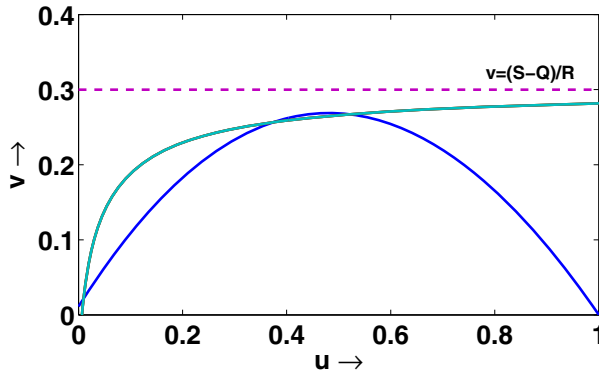
Equilibria

The boundary equilibrium points of the system are $E_0(0, 0)$ and $E_1(1, 0)$. The interior equilibrium points are the intersection points of the system (3)–(4) in the interior of the first quadrant.

From Eq. (3), we get

$$(1 - u) = \frac{\alpha v}{A + u + Bv},$$
$$(1 - u)(A + u + Bv) = \alpha v,$$
$$v = \frac{(u + A)(u - 1)}{B - Bu - \alpha}.$$

From Eq. (4), we get

$$\frac{Su}{A + u + Bv} = Q + Rv,$$
$$Su = (Q + Rv)(A + u + Bv),$$

Fig. 1 The blue coloured curve is the first nullcline. The purple coloured doted line is the horizontal asymptote of the second nullcline (cyan blue coloured curve)

$$v^2(-RB) - v(BQ + AR + Ru) + (Su - Qu - AQ) = 0,$$

$$v = \frac{BQ + AR + Ru \pm \sqrt{(BQ + AR + Ru)^2 + 4RB(Su - Qu - AQ)}}{-2RB}.$$

So, interior equilibrium points of the system (3)–(4) are the intersection points of the following two nullclines

$$v = \frac{(u + A)(u - 1)}{B - Bu - \alpha}, \tag{5}$$

$$v = \frac{BQ + AR + Ru - \sqrt{(BQ + AR + Ru)^2 + 4RB(Su - Qu - AQ)}}{-2RB}. \tag{6}$$

We take square root negative in the Eq. (6), if the square root positive then $v < 0$, so we do not get any branch in the positive quadrant. First nullcline (5) (see Fig. 1, blue coloured curve) is a continuous smooth curve and lies in the first quadrant for $u \in [0, 1]$. The curve is increasing at $(0, 0)$ and decreasing at $(1, 0)$ and attains a local maximum at $u_m = \frac{(\alpha - \alpha) + \sqrt{(\alpha - B)^2 - B(\alpha A + B - \alpha)}}{B}$ such that $0 < u_m < 1$. The cyan blue coloured second nullcline (6) intersects the positive u-axis at $\left(\frac{AQ}{S-Q}, 0\right)$ and then rises monotonically and bounded by its horizontal asymptote $v = \frac{S-Q}{R}$ (see Fig. 1). We assume the parametric restriction $S > Q$ because if $S < Q$, then the second nullcline has no branch in the first quadrant of the uv-plane and so the system have no feasible interior equilibrium point.

Theorem 3.1 *Let us assume $S > Q$ holds.*

(a) *If $Q(1+A) < S$ then the system can have either one interior equilibrium or three interior equilibrium points.*
(b) *If $S < Q(1 + A)$ then the system does not posses any feasible interior equilibrium point.*

Proof If we denote interior equilibrium point by $E_{i*}(u_{i*}, v_{i*})$ ($i = 1, 2, 3$, as number of interior equilibrium varies from one to three), then u_{i*} and v_{i*} are the positive root of

$$v = \frac{(u + A)(u - 1)}{B - Bu - \alpha}, \tag{7}$$

$$F_2(u) = Mu^3 + Nu^2 + Ou + P = 0, \tag{8}$$
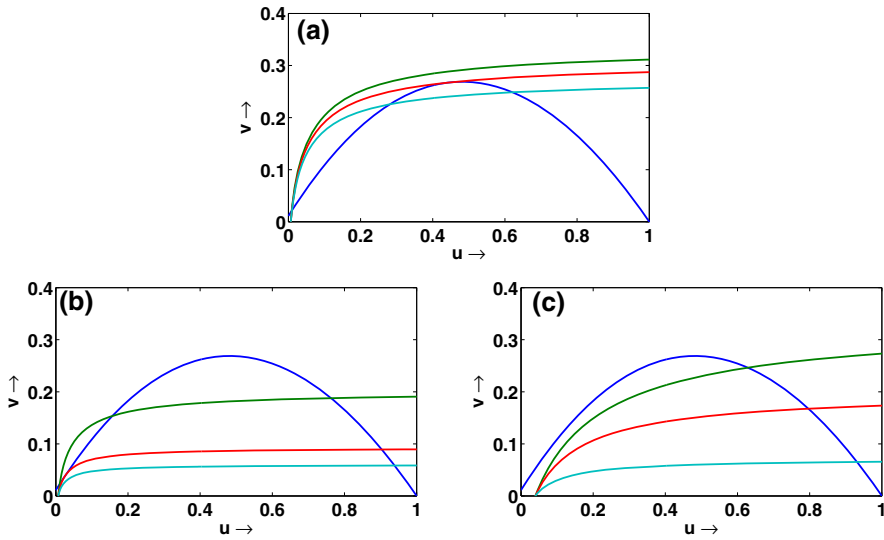
Fig. 2 Possible number of equilibrium points changes from one to three. [parameters: $\alpha = 1$, $A = 0.01$, $B = 0.1$, $Q = 0.2$, **a** $S = 0.5$, $R_{SN_1} = 0.9794387$, **b** $S = 0.5$, $R_{SN_2} = 3.243718$, **c** $S = 0.25$]

where $M = B^2 S + \alpha R$, $N = 2\alpha B S + 2\alpha A R - 2B^2 S - \alpha B Q - \alpha R$, $O = B^2 S - 2\alpha B S + \alpha B Q - \alpha A B Q + \alpha^2 S - \alpha^2 Q + \alpha A^2 R - 2\alpha A R$ and $P = \alpha A B Q - \alpha^2 A Q - \alpha A^2 R$. It is quite difficult to find the intersection points by solving analytically. so we can try to find the intersection points geometrically which is represented in Fig. 2.

If $Q(1 + A) < S$ holds then the point $\left(\frac{AQ}{S-Q}, 0\right)$ lies in between $(0, 0)$ and $(1, 0)$, the number of points of intersection of the two curves (7) and (8) changes from one to three if we gradually increase the value of R keeping all other parameters fixed. We assume the u-components of the interior equilibria satisfy the ordering $0 < u_{1*} < u_{2*} < u_{3*} < 1$ whenever they exist. Figure 2 illustrates the possible number of interior equilibrium points under the parametric restriction $Q(1 + A) < S$ when R varies. We can find a value of S, denoted by S_*, for which unique interior equilibrium point exists under the restriction $Q(1 + A) < S < S_*$. When $S_* < S$, one or three interior equilibrium points exist depending upon R. For any fixed value of S ($S_* < S$), we find a critical value of $R = R_{SN_1}$ (see Fig. 2a) for which the number of interior equilibrium points changes from one to three. The system admits three interior equilibrium points when $R_{SN_1} < R < R_{SN_2}$ holds. Here $R = R_{SN_2}$ (see Fig. 2b) is the threshold at which E_{1*} and E_{2*} collide and one more saddle-node bifurcation occurs. Then E_{1*} and E_{2*} disappears and the system continues to have one interior equilibrium point for all $R > R_{SN_2}$ (see Fig. 2c).

If $S < Q(1 + A)$ then the point $\left(\frac{AQ}{S-Q}, 0\right)$ lies on the right side of $(1, 0)$, the system has no feasible interior equilibrium point. $\qquad\square$

Local Stability Results of the Equilibria

In this section we discuss the local stability property of the equilibrium points. First we check the stability property of trivial and boundary equilibria.

Proposition 1 *(a)* $E_0(0, 0)$ *is always a saddle point.*
(b) $E_1(1, 0)$ *is a stable point if* $S < Q(1 + A)$ *and a saddle point if* $S > Q(1 + A)$.
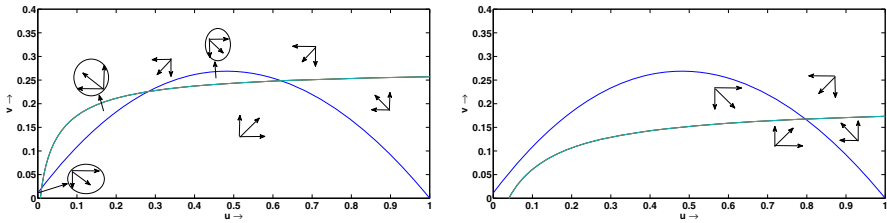
Fig. 3 Nature of stability of the interior equilibrium points

Proof The Jacobian matrix of the system is given by

$$J = \begin{pmatrix} F_u & F_v \\ G_u & G_v \end{pmatrix},$$

where $F(u, v) = u(1 - u) - \frac{\alpha uv}{A+u+Bv}$, $G(u, v) = \frac{Suv}{A+u+Bv} - Qv - Rv^2$ and $F_u = 1 - 2u - \frac{\alpha v(A+Bv)}{(A+u+Bv)^2}$, $F_v = -\frac{\alpha u(A+u)}{(A+u+Bv)^2}$, $G_u = \frac{Sv(A+Bv)}{(A+u+Bv)^2}$, $G_v = \frac{Su(A+u)}{(A+u+Bv)^2} - Q - 2Rv$.

Evaluating the Jacobian matrix at E_0 and E_1 we find,

$$J_{E_0} = \begin{pmatrix} 1 & 0 \\ 0 & -Q \end{pmatrix}, \quad J_{E_1} = \begin{pmatrix} -1 & -\frac{\alpha}{1+A} \\ 0 & \frac{S}{1+A} - Q \end{pmatrix}.$$

The eigenvalues of J_{E_0} are 1 and $-Q$, so $E_0(0, 0)$ is always a saddle point. The eigenvalues of J_{E_1} are -1 and $\frac{S}{1+A} - Q$, so $E_1(1, 0)$ is a stable point if $S < Q(1 + A)$ and a saddle point if $S > Q(1 + A)$. $\qquad\square$

Remark We have two cases. When $S < Q(1 + A)$, then no interior equilibrium point exists but $E_1(1, 0)$ is stable. When $S > Q(1+A)$, then interior equilibrium points exist but $E_1(1, 0)$ is saddle.

It is quite difficult to find the stability nature of the interior equilibrium points analytically. Hence we study the general nature of the two nullclines with direction of their vector fields and graphical Jacobian [Hastings, 1997] to find the nature of the stability of the interior equilibrium points.

Proposition 2 *Let us assume $S > Q$ holds.*

(a) E_{1*}, *is an unstable point whenever it exists.*
(b) E_{2*}, *is a saddle point whenever it exists.*
(c) E_{3*}, *is locally asymptotically stable (unstable) if $Tr J_{E_{3*}} < 0$ ($Tr J_{E_{3*}} > 0$).*

Proof Let $F(u, v) = uf(u, v)$ and $G(u, v) = vg(u, v)$ with $f(u, v) = (1 - u) - \frac{\alpha v}{A+u+Bv}$ and $g(u, v) = \frac{Su}{A+u+Bv} - Q - Rv$. Then we can write,

$$J_{E_{i*}} = \begin{pmatrix} F_u & F_v \\ G_u & G_v \end{pmatrix} = \begin{pmatrix} uf_u & uf_v \\ vg_u & vg_v \end{pmatrix}.$$

Using the graphical Jacobian method we find,

$$Sign(J_{E_{3*}}) = Sign \begin{pmatrix} uf_u & uf_v \\ vg_u & vg_v \end{pmatrix} = \begin{pmatrix} - & - \\ + & - \end{pmatrix}, u_{3*} > u_{f_{max}}$$

$$= \begin{pmatrix} + & - \\ + & - \end{pmatrix}, u_{3*} < u_{f_{max}},$$

where $u_{f_{max}}$ is the maximum of the curve f(u,v)=0. For $u_{3*} > u_{f_{max}}$, E_{3*}, is locally asymptotically stable as $Det(J_{E_{3*}}) > 0$ and $Tr J_{E_{3*}} < 0$. Now if $u_{3*} < u_{f_{max}}$, we have $\frac{dv^f}{du}|_{E_{3*}} < \frac{dv^g}{du}|_{E_{3*}}$, which implies $Det(J_{E_{3*}}) > 0$, so E_{3*} is stable if $Tr J_{E_{3*}} < 0$ and unstable if $Tr J_{E_{3*}}) > 0$ (Fig. 3).

Next whenever E_{2*} exists we have,

$$Sign(J_{E_{2*}}) = Sign \begin{pmatrix} uf_u & uf_v \\ vg_u & vg_v \end{pmatrix} = \begin{pmatrix} + & - \\ + & - \end{pmatrix}.$$

But in this case $\frac{dv^f}{du}|_{E_{2*}} > \frac{dv^g}{du}|_{E_{2*}}$, which implies $Det(J_{E_{2*}}) < 0$, so E_{2*}, is always a saddle point (Fig. 3).

E_{1*} is always unstable whenever it exists. It is quite difficult to determine analytically and graphically, so we can ensure it by numerical simulations. For example if we fix the parameters $\alpha = 1$, $A = 0.01$, $B = 0.1$, $Q = 0.2$, $R = 3.2$ and $S = 0.5$, then we have three interior equilibrium points namely $E_{1*}(0.02288852440, 0.03561581696)$, $E_{2*}(0.03205029891, 0.04506460096)$, $E_{3*}(0.9016914419, 0.09051692997)$. The eigenvalues of the Jacobian matrix calculated at E_{1*} are 0.402426653309752 and 0.0436043590902483, which confirms that E_{1*} is unstable.   □

Local Bifurcations

In this section we study several local bifurcations, namely, transcritical bifurcation, saddle-node bifurcation, Hopf-bifurcation; which are of codimension one and the system also undergoes different types of codimension two bifurcations, namely, cusp bifurcation, Bogdanov–Takens bifurcation and Bautin bifurcation. We assume that $S > Q$, otherwise the interior equilibrium points does not exist.

Theorem 3.2 *The model system go through a transcritical bifurcation at* $E_1(1, 0)$ *when the parameter S crosses the transcritical bifurcation threshold* $S_{TC} = Q(1 + A)$.

Proof We prove that one interior equilibrium point bifurcates from $(1, 0)$ at the threshold $S = Q(1 + A) = S_{TC}$ through transcritical bifurcation and also check the transversality condition for transcritical bifurcation according to the Sotomayer's theorem [29].

Calculating the jacobian matrix of the system (3)–(4) at $(1, 0)$ when $S = S_{TC}$, we find det $J|_{S_{TC}} = 0$. So zero is an eigenvalue of the matrix. The eigenvectors corresponding to zero eigenvalue of $J_{S_{TC}}$ and $[J_{S_{TC}}]^T$ are $V = [-\frac{\alpha Q}{S}, 1]^T$ and $W = [0, 1]^T$ respectively. Now we check the transversality conditions,

$$W^T F_{1S}((1, 0); S_{TC}) = 0,$$

$$W^T DF_{1S}((1, 0); S_{TC})V = \frac{1}{1 + A} \neq 0,$$

$$W^T D^2 F_1((1, 0); S_{TC})(V, V) = -2 \left[\frac{AQ\alpha}{(1 + A)^2} + \frac{BQ}{(1 + A)} + R \right] < 0,$$

where $F_1(u, v) = [F(u, v), G(u, v)]^T$ and $F_{1S}(u, v) = \left[\frac{\partial F}{\partial S}(u, v), \frac{\partial G}{\partial S}(u, v) \right]^T$ (for details see Appendix 1). Here the transcritical bifurcation is supercritical and one interior equilibrium point is generated through this transcritical bifurcation.   □

Theorem 3.3 *The system go through saddle-node bifurcation when* $F_2(u) = 0$ *has a double root in the interval* $(0, 1)$.

Proof Let u_{SN*} be a double root of $F_2(u) = 0$ such that $0 < u_{SN*} < 1$. Let us define the corresponding threshold for S by S_{SN} and for $S = S_{SN}$ we find u_{SN*} is a double root of $F_2(u) = 0$. Then the two nullclines (5–6) touch each other at $(u_{SN*}, v_{SN*}) = E_{SN*}$ (say). As, $F(u, v) = uf(u, v)$ and $G(u, v) = vg(u, v)$ and slopes of the both curves are equal at E_{SN*}, i.e., $\frac{dv^f}{du} = \frac{dv^g}{du}$. Since $\frac{dv^f}{du} = \frac{\partial F/\partial u}{\partial F/\partial v}$ and $\frac{dv^g}{du} = \frac{\partial G/\partial u}{\partial G/\partial v}$ we have det $J_{E_{SN*}} = 0$ and hence the Jacobian matrix has a zero eigenvalue with multiplicity one. Now eigenvectors corresponding to zero eigenvalue of $J_{E_{SN*}}$ and $[J_{E_{SN*}}]^T$ are $V = (1, k')^T$ and $W = (k'', 1)^T$ respectively, where $k' = -\frac{Su(A+Bv)}{Su(A+u)-(Q+2Rv)(A+u+Bv)^2}$ and $k'' = \frac{Su(A+u)-(Q+2Rv)(A+u+Bv)^2}{\alpha u(A+u)}$. We verify the transversality conditions for saddle-node bifurcation [29]

$$W^T F_{1S}(E_{SN*}; S_{SN}) = \frac{uv}{A+u+Bv} \mid_{E_{SN*}} \neq 0,$$

$W^T D^2 F_1(E_{SN*}; S_{SN})(V, V) = \frac{2}{(A+u+Bv)^3}[-(A+u+Bv)^3 k'' + \alpha v(A+Bv)k'' - \alpha(A+u+Bv)(A+2Bv)k'k'' + \alpha Bv(A+Bv)k'k'' + \alpha Bu(A+u)k'^2 k'' - Sv(A+Bv) + S(A+u+Bv)(A+2Bv)k' - SBv(A+Bv)k' - Su(A+u)k'^2 - R(A+u+Bv)^3 k'^2] \neq 0$ (If $S \neq S_{CP}, R \neq R_{CP}$)

(for details see "Appendix 2"). Hence the system undergoes saddle-node bifurcation. □

There exist two different cases of saddle-node bifurcation, one for the coincidence of E_{2*} and E_{3*} and the another one for the coincidence of E_{1*} and E_{2*}. Two saddle-node bifurcation curves are denoted by SN_1 and SN_2 respectively. The expression for the saddle-node bifurcation curves in $S - R$ plane, defined as function of u_{SN*}, is given below

$$F_2(u_{SN*}) = Mu_{SN*}^3 + Nu_{SN*}^2 + Ou_{SN*} + P = 0, \tag{9}$$

$$F_2'(u_{SN*}) = 3Mu_{SN*}^2 + 2Nu_{SN*} + O = 0. \tag{10}$$

Theorem 3.4 *The system will go through cusp bifurcation when $F_2(u) = 0$ has a triple root in the interval* $(0, 1)$.

Proof Let u_{CP*} be a triple root of $F_2(u) = 0$. Then its explicit expression is given by

$$u_{CP*} = -\frac{N}{3M} \tag{11}$$

For the feasibility of the point (u_{CP*}, v_{CP*}) the additional parametric restriction $\frac{N}{M} < 0$

Now proceeding as above it can be shown that the Jacobian matrix $J_{E_{CP*}}$ at $E_{CP*}(u_{CP*}, v_{CP*})$ has one zero eigenvalue. Also, the quadratic normal form coefficient is given by,

$$W^T D^2 F_1(E_{CP*}; S_{CP})(V, V) = 0.$$

Thus the system exhibit a codimension two local bifurcation namely cusp bifurcation when the parameters (S, R) cross the threshold (S_{CP}, R_{CP}). Thus in the cusp bifurcation point both saddle-node bifurcation curves SN_1 and SN_2 meet each other. For finding the expression of (S_{CP}, R_{CP}) we replace the value of u_{SN*} by u_{CP*} in (9)–(10). □

Now we discuss the stability change of the interior equilibrium points through Hopf-bifurcation. Only one interior point E_{3*} changes its stability. The result is stated in the following theorem.

Theorem 3.5 *The interior equilibrium point E_{3*} changes its stability through Hopf-bifurcation at the threshold $S = S_H = \frac{1}{u(A+u)}[\alpha v(A+Bv) - (1-2u-Q-2Rv)(A+u+Bv)^2]$ such that $Tr(J_{E_{3*}}) \mid_{S=S_H} = 0$ and $\frac{d}{dS}[Re(\lambda)] \mid_{S=S_H} \neq 0$, where λ is an eigenvalue of the Jacobian matrix $J_{E_{3*}}$ at $S = S_H$.*
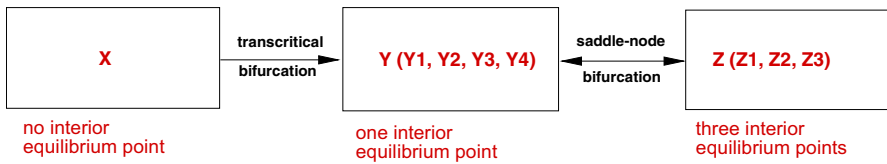
Three domains X, Y and Z

Fig. 4 Three different domains

For $S = S_H$, clearly $Tr(J_{E_{3*}}) = 0$. It is quite difficult to find the nature of the limit cycle explicitly. The Hopf-bifurcation is called supercritical or subcritical if the Hopf-bifurcation limit cycle is stable or unstable respectively. Here we show numerically that the system undergoes Hopf-bifurcation. We fix the parameters $A = 0.01$, $B = 0.1$, $Q = 0.2$, $\alpha = 1$. Now for $R = 0.02$, $S = S_H = 0.22138829$, first lyapunov coefficient is $0.02455789 > 0$, so the system undergoes a subcritical Hopf-bifurcation and for $R = 0.01$, $S = S_H = 0.2184418$, first lyapunov coefficient is $-0.2869109 < 0$, so the system undergoes a supercritical Hopf-bifurcation.

Between supercritical and subcritical Hopf-bifurcation, we can find a value of S, R where first lyapunov coefficient is zero. At this point one more codimension two bifurcation occur and is called Bautin bifurcation. For $R = 0.019207$, $S = 0.2211546$, first lyapunov coefficient is zero.

Theorem 3.6 *The interior equilibrium point E_{3*} is go through a Bautin bifurcation when it undergoes Hopf-bifurcation such that first lyapunov coefficient is zero for some $R = R_{GH}$ and $S = S_{GH}$.*

Theorem 3.7 *The unique interior point $E_{BT*} = (u_{BT*}, v_{BT*})$ arising through saddle-node bifurcation, when E_{2*} and E_{3*} coincide, undergoes Bogdanov–Takens bifurcation at the threshold (S_{BT}, R_{BT}) if $\det J_{E_{BT*}} |_{(S_{BT}, R_{BT})} = 0$ and $Tr(J_{E_{BT*}}) |_{(S_{BT}, R_{BT})} = 0$.*

Proof At the (S_{BT}, R_{BT}) point in the $S - R$ plane $\det J_{E_{BT*}} |_{(S_{BT}, R_{BT})} = 0$ and $Tr(J_{E_{BT*}}) |_{(S_{BT}, R_{BT})} = 0$. So, we find the expression for (S_{BT}, R_{BT}) by replacing u_{SN*} by u_{BT*} in (9)–(10) and (u_{BT*}, v_{BT*}) in $Tr(J) = 0$. Again since explicit expressions for the component of the equilibrium points are hard to find out it is quite difficult to determine the analytical expression for the threshold of the Bogdanov–Takens bifurcation explicitly. We fix the parameters $A = 0.01$, $B = 0.1$, $Q = 0.2$, $\alpha = 1$ and for $R_{BT} = 0.3649024493$, $S = S_{BT} = 0.3223696400$, $\det J_{E_{BT*}} |_{(S_{BT}, R_{BT})} = 0$ and $Tr(J_{E_{BT*}}) |_{(S_{BT}, R_{BT})} = 0$. Again $\left(F_{uu} - \frac{F_u F_{uv}}{F_v} + G_{uv}\right) = -2.10254$ and $\left(0.5F_u F_{uu} - \frac{F_u^2 F_{uv}}{F_v} + 0.5F_v G_{uu} - F_u G_{uv}\right) = -0.385426$ prove the transversality conditions [20]. □

Global Dynamics

Local bifurcations are already discussed in the previous section under some parametric restrictions. Here we show the bifurcation diagram in $S - R$ plane to understand different regions and their dynamic behaviors. Transcritical and saddle-node bifurcation curves divide the plane into three different domains X, Y and Z among which no interior point for $(S, R) \in$

X, one interior point for $(S, R) \in Y \equiv \bigcup_{i=1}^{4} Y_i$, three interior point for $(S, R) \in Z \equiv \bigcup_{i=1}^{3} Z_i$ (see Fig. 4).

Schematic bifurcation diagram is shown in Fig. 5 and one can check this type of diagram for the system (3)–(4). Yellow coloured transcritical bifurcation curve TC passing through the point $(Q(1 + A), 0)$ vertically. In the parametric domain $S < Q(1 + A)$, denoted by X, no interior equilibrium point exists. At $S = Q(1 + A)$ one interior point E_{3*} appear through transcritical bifurcation TC as S enters the domain Y. Now if we increase the value of S still $S = S_{CP}$ the system will continued to have only one interior equilibrium point for any value of R. Next for fixed $R(> R_{CP})$ if we gradually increase the value of S firstly two more interior equilibrium points E_{1*} and E_{2*} appear through saddle-node bifurcation (SN_2) (cyan blue curve) as S goes from the region Y to Z. Again if we increase the value of S then interior equilibrium points E_{2*} and E_{3*} disappear through saddle-node bifurcation (SN_1) (blue coloured curve) as S enters the domain Y_4.
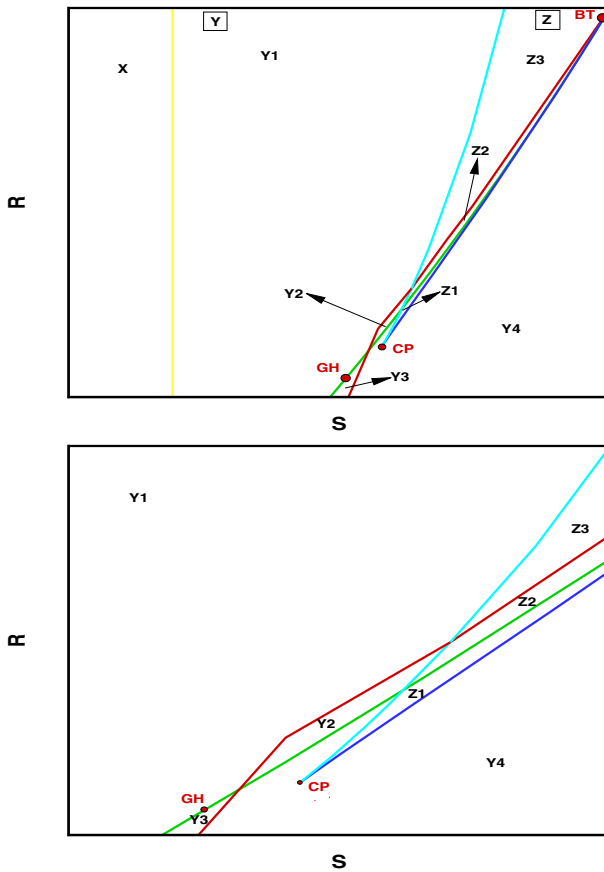
The saddle-node bifurcation curve (SN_1) passing through the BT point. The Hopf-bifurcation curve (green coloured curve) and a red coloured global bifurcation curve starts from this point. This global bifurcation curve is homoclinic bifurcation curve until it intersects the saddle-node bifurcation curve (SN_2). Four local bifurcation curves (one transcritical, two saddle-node and one Hopf-bifurcation curves) and global bifurcation curves divide the $S - R$ plane into several regions and we find different phase portraits for this domains.

Now we discuss the phase portraits and for this we fixed the parameters $A = 0.01$, $B = 0.1$, $\alpha = 1$, $Q = 0.2$ and varying the parameters S and R. $S_{TC} = 0.202$ is the transcritical bifurcation threshold and two saddle-node bifurcation curves intersect at the cusp bifurcation point $(S_{CP}, R_{CP}) = (0.2607806335, 0.1594581749)$. For fixed $S = 0.5$, two saddle-node bifurcation threshold is given by $R_{SN_1} = 0.9794387$ and $R_{SN_2} = 3.243718$ respectively. The Bogdanov–Takens bifurcation(BT) point is $(S_{BT}, R_{BT}) = (0.3223696400, 0.3649024493)$. Between supercritical and subcritical Hopf-bifurcation, we find a Bautin bifurcation threshold $R_{GH} = 0.019207$, $S_{GH} = 0.2211546$. Now we choose values of S and R from different domains in Fig. 5 such that we get different phase portraits (Figs. 6, 7). Number of interior equilibrium points varies from one to three but only one of them may asymptotically stable. We summarize existence, stability, limit cycles of the equilibrium points at Table 1.

Comparison with Our System (3)–(4) with [11]

In this subsection we have made the significant comparison of our proposed prey–predator model (3)–(4) with the model considered by Dimitrov and Kojouharov in [11]. In [11], Dimitrov and Kojouharov considered a linear predator–prey model with Beddington–DeAngelis functional response and linear intrinsic growth rate of the prey population and also neglect the density dependent death rate of predator. But our proposed model (3)–(4) is a non-linear predator–prey model with Beddington–DeAngelis functional response, where the density dependent death rate of predator is considered. We observed that the density dependent death rate parameter R has significant effects on the dynamics of the system. Comparing the dynamics of [11] with our proposed model we find the following differences:

1. Dimitrov and Kojouharov [11] has only two equilibria whereas our system has at most five equilibria.
2. In [11], origin is the only boundary equilibrium point of the system and it is unstable but our system has two boundary equilibrium points $E_0(0, 0)$ and $E_1(1, 0)$. In the absence of interior equilibria in our system, $E_1(1, 0)$ is not only locally asymptotically stable but

Fig. 5 Schematic bifurcation diagram in S-R plane (upper) and enlarge version (lower). Vertical yellow line is the transcritical bifurcation curve. Two saddle-node bifurcation curves (SN_2)(cyan blue) and (SN_1)(blue) meet at CP point. The green coloured Hopf-bifurcation curve and red coloured homoclinic bifurcation curve start from BT point. GH is the Bautin bifurcation point

also globally asymptotically stable, which can be verified from Fig. 6a though the origin is saddle point.

3. Dimitrov and Kojouharov's model has unique interior equilibrium point, which may be stable or unstable depending upon food weighting factor and conversion efficiency. Our system has at most three interior equilibrium points, one is unstable, one is saddle and one equilibrium point changes its stability through Hopf-bifurcation. In some regions stable interior equilibrium point is also globally asymptotically stable (see Fig. 6b). The Hopf-bifurcation was studied thoroughly in our model though it was not studied in [11].

4. In our model number of interior equilibrium point changes from one to three and again three to one via saddle-node bifurcation curve 2 (SN_2) and saddle-node bifurcation curve 1 (SN_1) respectively, and intersection point of this two curves gives cusp bifurcation. This type of scenario was not seen in [11].

5. In [11], limit cycle may appear around interior equilibrium point depending upon some parametric conditions but in our model limit cycle is observed clearly and also it is found that it can change it's stability through Bautin bifurcation.
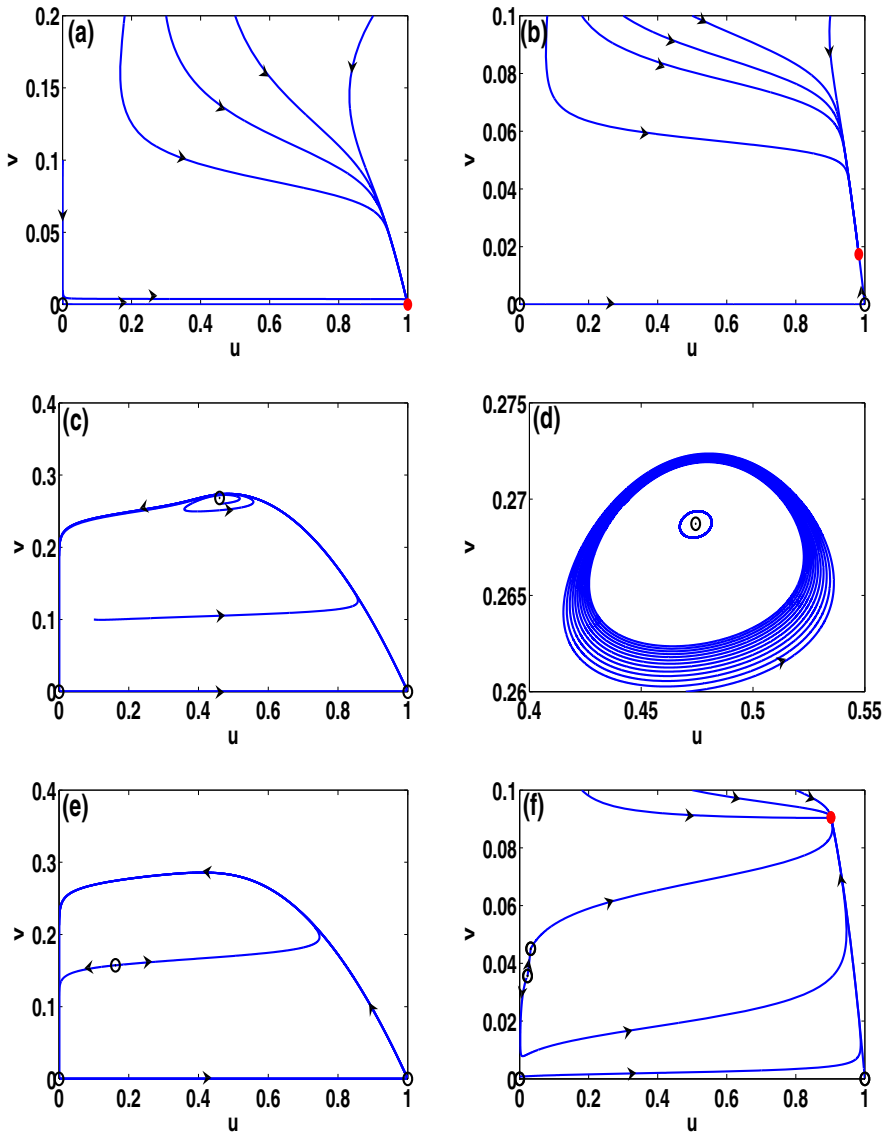
Fig. 6 Phase portrait for $\alpha = 1$, $A = 0.01$, $B = 0.1$, $Q = 0.2$ and varies S and R. **a** $S = 0.2$, $R = 1$ (domain X), **b** $S = 0.22$, $R = 1$ (domain Y_1), **c** $S = 0.2449734564$, $R = 0.1$ (domain Y_2), **d** $S = 0.2184419$, $R = 0.01$ (domain Y_3), **e** $S = 0.25$, $R = 0.1$ (domain Y_4), **f** $S = 0.5$, $R = 3.2$ (domain Z_3)

6. In our model solutions of the system (3)–(4) are always bounded but In [11], when maximum growth rate of predator is very small then all trajectories are unbounded.
7. The existence of more than one interior equilibrium point in our model is due to density dependent death rate and also when density dependent death rate is very high, we found stable coexisting steady-state.
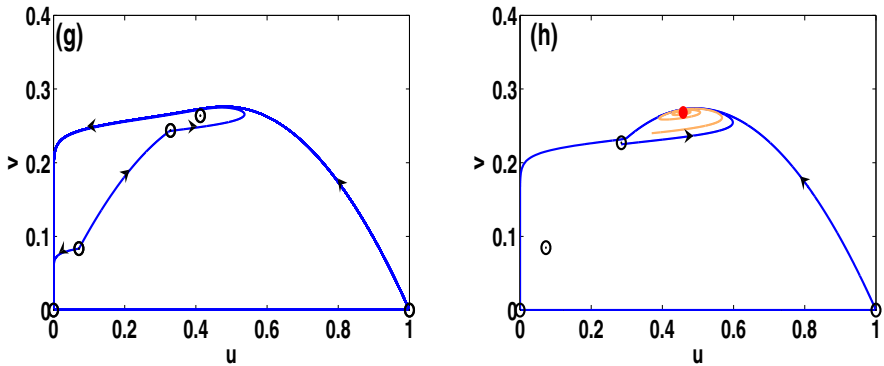
Fig. 7 Phase portrait for $\alpha = 1$, $A = 0.01$, $B = 0.1$, $Q = 0.2$ and varies S and R. **g** $S = 0.2707212629$, $R = 0.185$ (domain Z_1), **h** $S = 0.2707212629$, $R = 0.18863$ (domain Z_2)

Table 1 Number and nature of the equilibrium points which described in bifurcation diagram (Fig. 5)

Domain	Number of Interior equilibrium point	Nature of the phase portrait
X	Nil	E_1 is locally asymptotically stable and E_0 is saddle point
Y_1	E_{3*} exists	E_{3*} is locally asymptotically stable, E_0 and E_1 are saddle points
Y_2	E_{3*} exists	E_{3*} is stable surrounded by an unstable limit cycle, E_0 and E_1 are saddle points
Y_3	E_{3*} exists	E_{3*} is unstable surrounded by a stable limit cycle, E_0 and E_1 are saddle points
Y_4	E_{3*} exists	E_{3*} is unstable point, E_0 and E_1 are saddle points
Z_1	E_{1*}, E_{2*} and E_{3*} exist	E_{1*}, E_{3*} are unstable points, E_{2*} is saddle point, E_0 and E_1 are saddle points
Z_2	E_{1*}, E_{2*} and E_{3*} exist	E_{3*} is a stable point surrounded by an unstable limit cycle, E_{1*} is unstable, E_{2*} is saddle point, E_0 and E_1 are saddle points
Z_3	E_{1*}, E_{2*} and E_{3*} exist	E_{3*} is a stable point, E_{1*} is unstable, E_{2*} is saddle point, E_0 and E_1 are saddle points

Discussion

In the previous section we have presented the effect of density dependent death rate and conversion rate in our standard prey–predator model with Beddington–DeAngelis functional response and logistic growth rate for the prey population. Not only this but also death rate of predator has a great impact in the system. When death rate of predator is very high and conversion rate is low then predator can not survive and prey population stabilize globally at the level of their carrying capacity (Prop. 1-(b)). When death rate of predator is low then the predator has a chance to survive and both prey and predator populations may coexist (Thm. 3.1). It is very difficult to find the explicit expression for the coexistence of the prey and predator but bifurcation analysis give us the implicit parametric restrictions to verify both

coexistence and stability properties. The summarized result are at Table 1. Origin is always a saddle point. The existence of more than one interior equilibrium points is due to density dependent death rate but at most one of the interior equilibrium points is stable. Hence the stable coexisting steady-state is only one and it depends on the initial population densities. When death rate of predator is not high it may be possible that neither prey population nor predator species are stable depends upon the density dependent death rate and conversion rate. When density dependent death rate is very high then we found stable coexisting steady-state. From the phase portraits in Figs. 6 and 7, it is clear that magnitude of parameters decide the basin of attraction of the stable equilibrium point. One more important dynamic is oscillatory coexistence and it is also possible for both populations. Stable coexistence of both prey and predator populations may be destroyed by increasing the conversion rate. There exist a balance between prey and predator and we get a periodic behavior for a long term prediction. When density dependent death rate is very low then we get stable oscillatory coexistence otherwise we get unstable limit cycle which acts as a separatrix of the domain of attraction of coexistence state.

A comparison of our proposed prey–predator model (3)–(4) with the model considered by Dimitrov and Kojouharov in [11] have been discussed in "Comparison with our system (3)–(4) with [11]" section. We have found that logistic prey growth and density dependent death rate of predator make the system more complicated. There are several local and global bifurcations occur, local bifurcation curves in bifurcation diagram describe the change in number of equilibrium points and their stability and on the other hand global bifurcation curves describe the extreme change in the system dynamics. When the parameters enters from domain Z_2 to domain Z_3 then homoclinic bifurcation occurs and the stable limit cycle disappears and as a result both the populations stabilize at the interior equilibrium point and this equilibrium is globally stable.

The present model can be generalized to further complex models which can be studied in future. Now we discuss some of the issues which may be taken care of to extend the present model.

Environmental fluctuations or demographic stochasticity into the modelling approach, which are important components for ecosystems exposed within open environment. In deterministic modelling approach, we always assume that parameters involved in the system are absolute constant irrespective of the environmental periodicity and fluctuations. But in reality, parameters involved in the system always fluctuate around some average value due to continuous fluctuation in the environment. May [25] pointed out that all the parameters involved in the population model exhibit random fluctuation as the factors controlling them are not constant. Hence equilibrium distributions obtained from the deterministic analysis are not realistic rather they fluctuate randomly around some average value. Sometimes, a large amplitude fluctuation is observed in the population density which leads to extinction of certain species. Therefore, in order to study the dynamics of interacting population under realistic situation, we need to corporate the effect of environmental fluctuations in the deterministic model by considering the associated stochastic differential equation model (noise added model). Hence, it will be interesting to study the effect of environmental fluctuations in the given ecological model by extending the model into a stochastic differential equation model in future.

On the other hand, researchers have drawn their attention towards the epidemiological models including feedback control variables from the last few years [7,32,33,40] as this variable capture the unpredictable disturbances and uncertain environments in realistic situations. But very few ecological models have been investigated using such control techniques [26,40]. Hence, we leave this ecological model with feedback control variable for future

study. Also we know that time delay plays an important role to stabilize or destabilize the coexistence steady-state arising in several preypredator models [1,4,15,17,24,31]. Hence, it would be better to study the proposed prey–predator model with time delay also.

A Appendix 1

Transversality conditions for transcritical bifurcation: We check the first transversality condition, $F_1(u, v) = [F(u, v), G(u, v)]^T$ and $F_{1S}(u, v) = \left[\frac{\partial F}{\partial S}(u, v), \frac{\partial G}{\partial S}(u, v)\right]^T = \left[0, \frac{uv}{A+u+Bv}\right]^T$. Now $W^T F_{1S}(u, v) = \begin{pmatrix} 0 & 1 \end{pmatrix} \begin{pmatrix} 0 \\ \frac{uv}{A+u+Bv} \end{pmatrix} = \frac{uv}{A+u+Bv}$. So we get $W^T F_{1S}((1, 0); S_{TC}) = 0$.

Second transversality condition,

$$DF_{1S}V = \begin{pmatrix} \frac{\partial F_S}{\partial u}v_1 & \frac{\partial F_S}{\partial v}v_2 \\ \frac{\partial G_S}{\partial u}v_1 & \frac{\partial G_S}{\partial v}v_2 \end{pmatrix} = \begin{pmatrix} 0 \\ \frac{(Av+Bv^2)(\alpha Q)}{(A+u+Bv)^2 S} + \frac{(Au+u^2)}{(A+u+Bv)^2} \end{pmatrix}.$$

So $DF_{1S}((1, 0); S_{TC})V = \begin{pmatrix} 0 \\ \frac{1}{1+A} \end{pmatrix}$ and $W^T DF_{1S}((1, 0); S_{TC})V = \frac{1}{1+A} \neq 0$.

Third condition,

$$D^2 F_1(V, V) = \begin{pmatrix} F_{uu}v_1v_1 + F_{uv}v_1v_2 + F_{vu}v_2v_1 + F_{vv}v_2v_2 \\ G_{uu}v_1v_1 + G_{uv}v_1v_2 + G_{vu}v_2v_1 + G_{vv}v_2v_2 \end{pmatrix},$$

where $V = (v_1, v_2)^T$. At $(1, 0)$ point, $F_{uu} = -2$, $F_{uv} = -\frac{\alpha A(A+1)}{(A+1)^3} = F_{vu}$, $F_{vv} = \frac{2\alpha B(A+1)}{(A+1)^3}$ and $G_{uu} = 0$, $G_{uv} = \frac{SA(A+1)}{(A+1)^3} = G_{vu}$, $G_{vv} = -\frac{2BS(A+1)}{(A+1)^3} - 2R$.

We find the expression of $W^T D^2 F_1((1, 0); S_{TC})(V, V)$ as

$$\begin{pmatrix} 0 & 1 \end{pmatrix} \begin{pmatrix} -2\frac{(\alpha Q)^2}{S^2} + 2\frac{\alpha^2 QA(A+1)}{(A+1)^3 S} + \frac{2\alpha B(A+1)}{(A+1)^3} \\ -2\left[\frac{AQ\alpha}{(1+A)^2} + \frac{BQ}{(1+A)} + R\right] \end{pmatrix} = -2\left[\frac{AQ\alpha}{(1+A)^2} + \frac{BQ}{(1+A)} + R\right] < 0.$$

The system experiences a supercritical transcritical bifurcation and one interior equilibrium point is generated.

B Appendix 2

Transversality conditions for saddle-node bifurcation are given by

First transversality condition: $W^T F_{1S}(E_{SN*}; S_{SN}) \neq 0$.

$F_{1S}(u, v) = \left[0, \frac{uv}{A+u+Bv}\right]^T$ and $W^T F_{1S}(E_{SN*}; S_{SN}) = \frac{uv}{A+u+Bv} |_{E_{SN*}} \neq 0$, where $W = (k'', 1)^T$ and $k'' = \frac{Su(A+u) - (Q+2Rv)(A+u+Bv)^2}{\alpha u(A+u)}$.

Second transversality condition: $W^T D^2 F_1(E_{SN*}; S_{SN})(V, V) \neq 0$.

Now, $F_1(u, v) = [F(u, v), G(u, v)]^T$, where $F(u, v) = u(1 - u) - \frac{\alpha uv}{A+u+Bv}$, $G(u, v) = \frac{Suv}{A+u+Bv} - Qv - Rv^2$.

$$D^2 F_1(u, v)(V, V) = \sum_{i,j=1}^{2} \frac{\partial^2 F_1(u, v)}{\partial u_i \partial u_j} v_i v_j, \text{ where } (u, v) = (u_1, u_2)(\text{say}). \text{ Then,}$$

$$D^2 \begin{pmatrix} F(u, v) \\ G(u, v) \end{pmatrix} (V, V) = \begin{pmatrix} \displaystyle\sum_{i,j=1}^{2} \frac{\partial^2 F(u, v)}{\partial u_i \partial u_j} v_i v_j \\ \displaystyle\sum_{i,j=1}^{2} \frac{\partial^2 G(u, v)}{\partial u_i \partial u_j} v_i v_j \end{pmatrix}$$

$$= \begin{pmatrix} F_{u_1^2} v_1^2 + 2F_{u_1 u_2} v_1 v_2 + F_{u_2^2} v_2^2 \\ G_{u_1^2} v_1^2 + 2G_{u_1 u_2} v_1 v_2 + G_{u_2^2} v_2^2 \end{pmatrix},$$

where $V = (v_1, v_2)^T = (1, k')^T$ and $k' = -\frac{Su(A+Bv)}{Su(A+u)-(Q+2Rv)(A+u+Bv)^2}$, $F_{u_i u_j} = \frac{\partial^2 F}{\partial u_i \partial u_j}$ for $i, j = 1, 2$ and similarly for G. Using the equilibrium relation we get,

$$D^2 F_1(E_{SN*}; S_{SN})(V, V)$$
$$= \begin{pmatrix} -2 + 2\frac{\alpha v(A+Bv)}{(A+u+Bv)^3} - 2\frac{\alpha(A+u+Bv)(A+2Bv)-2\alpha Bv(A+Bv)}{(A+u+Bv)^3}k' + 2\frac{\alpha Bu(A+u)}{(A+u+Bv)^3}k'^2 \\ -2\frac{Sv(A+Bv)}{(A+u+Bv)^3} + 2\frac{S(A+u+Bv)(A+2Bv)-2SBv(A+Bv)}{(A+u+Bv)^3}k' - 2(\frac{Su(A+u)}{(A+u+Bv)^3} + R)k'^2 \end{pmatrix}.$$

We find the expression $W^T D^2 F_1(E_{SN*}; S_{SN})(V, V) = \frac{2}{(A+u+Bv)^3}[-(A + u + Bv)^3 k'' + \alpha v(A + Bv)k'' - \alpha(A + u + Bv)(A + 2Bv)k'k'' + \alpha Bv(A + Bv)k'k'' + \alpha Bu(A+u)k'^2 k'' - Sv(A + Bv) + S(A + u + Bv)(A + 2Bv)k' - SBv(A + Bv)k' - Su(A + u)k'^2 - R(A + u + Bv)^3 k'^2]$.

If $S \neq S_{CP}$, $R \neq R_{CP}$ then $W^T D^2 F_1(E_{SN*}; S_{SN})(V, V) \neq 0$. So the system undergoes saddle-node bifurcation.

References

1. Aiello, W.G., Freedman, H.I.: A time-delay model of single species growth with stage-structure. Math. Biosci. **101**, 139–153 (1990)
2. Bazykin, A.D., Khibnik, A.I., Krauskopf, B.: Nonlinear Dynamics of Interacting Populations, vol. 11. World Scientific Publishing, Singapore (1998)
3. Banerjee, M., Petrovskii, S.: Self-organised spatial patterns and chaos in a ratio-dependent predator–prey system. Theor. Ecol. **4**, 37–53 (2011)
4. Banerjee, M., Takeuchi, Y.: Maturation delay for the predators can enhance stable coexistence for a class of prey–predator models. J. Theor. Biol **412**, 154–171 (2016)
5. Beddington, J.R.: Mutual interference between parasites or predators and its effect on searching efficiency. J. Anim. Ecol. **44**, 331–340 (1975)
6. Cantrell, R.S., Cosner, C.: On the dynamics of predatorprey models with the Beddington–DeAngelis functional response. J. Math. Anal. Appl. **257**, 206–222 (2001)
7. Chen, L., Sun, J.: Global stability of an SI epidemic model with feedback controls. Appl. Math. Lett. **28**, 53–55 (2014)
8. Conway, E.D., Smoller, J.A.: Global analysis of a system of predator–prey equations. SIAM J. Appl. Math. **46**, 630–642 (1986)
9. Cosner, C., DeAngelis, D.L., Ault, J.S., Olson, D.B.: Effects of spatial grouping on the functional response of predators. Theor. Popul. Biol. **56**, 65–75 (1999)
10. DeAngelis, D.L., Goldstein, R.A., ONeill, R.V.: A model for trophic interaction. Ecology **56**, 881–892 (1975)
11. Dimitrov, D.T., Kojouharov, H.V.: Complete mathematical analysis of predator–prey models with linear prey growth and Beddington–DeAngelis functional response. Appl. Math. Comput. **162**, 523–538 (2005)

12. Freedman, H.: Stability analysis of a predator–prey system with mutual interference and density-dependent death rates. Bull. Math. Biol. **41**, 67–78 (1979)
13. Freedman, H.: Deterministic Mathematical Method in Population Ecology. Dekker, New York (1990)
14. Gonzalez-Olivares, E., Rojas-Palma, A.: Multiple limit cycles in a gause type predator-prey model with holling type III functional response and allee effect on prey. Bull. Math. Biol. **73**, 1378–1397 (2011)
15. Gourley, S.A., Kuang, Y.: A stage structured predator-prey model and its dependence on maturation delay and death rate. J. Math. Biol. **49**, 188–200 (2004)
16. Holling, C.: The functional response of predators to prey density and its role in mimicry and population regulation. Mem. Entomol. Soc. Can. **97**, 1–60 (1965)
17. Jankovic, M., Petrovskii, S.: Are time delays always destabilizing? Revisiting the role of time delays and the Allee effect. Theor. Ecol. **7**, 335–349 (2004)
18. Jost, C., Arino, O., Arditi, R.: About deterministic extinction in ratio-dependent predator-prey models. Bull. Math. Biol. **61**, 19–32 (1999)
19. Kuang, Y., Baretta, E.: Global qualitative analysis of a ratio-dependent predatorprey system. J. Math. Biol. **36**, 389–406 (1998)
20. Kuznetsov, Y.A.: Elements of Applied Bifurcation Theory. Springer, New York (2004)
21. Lahrouz, A., Settati, A., Mandal, P.S.: Dynamics of a switching diffusion modified LeslieGower predatorprey system with Beddington-DeAngelis functional response. Nonlinear Dyn. **85**, 853–870 (2016)
22. Liu, M., Wang, K.: Global stability of a nonlinear stochastic predatorprey system with Beddington–DeAngelis functional response. Commun Nonlinear Sci. Numer Simul. **16**, 1114–1121 (2011)
23. Lotka, A.J.: A Natural Population Norm I and II. Academy of Sciences, Washington (1913)
24. Martin, A., Ruan, S.: Predator–prey models with delay and prey harvesting. J. Math. Biol. **43**, 247–267 (2001)
25. May, R.M.: Stability and Complexity in Model Ecosystems. Princeton University Press, Princeton (2001)
26. Liao, X., Zhou, S., Chen, Y.: Permanence and global stability in a discrete n-species competition system with feedback controls. Nonlinear Anal. Real World Appl. **9**, 1661–1671 (2008)
27. Morozov, A., Petrovskii, S., Li, B.-L.: Spatiotemporal complexity of patchy invasion in a predator–prey system with the allee effect. J. Theor. Biol. **238**, 18–35 (2006)
28. McGehee, E.A., Schutt, N., Vasquez, D.A., Peacock-Lopez, E.: Bifurcations, and temporal and spatial patterns of a modified lotka-volterra model. Int. J. Bifurc. Chaos **18**, 2223–2248 (2008)
29. Perko, L.: Differential Equations and Dynamical Systems, vol. 7. Springer, New York (2000)
30. Sen, M., Banerjee, M.: Rich global dynamics in a prey–predator model with Allee effect and density dependent death rate of predator. Int. J. Bifurc. Chaos **25**(03), 1530007 (2015)
31. Sen, M., Banerjee, M., Morozov, A.: Stage-structured ratio-dependent predator–prey models revisited: when should the maturation lag result in systems destabilization? Ecol. Comp. **19**, 23–34 (2014)
32. Shang, Y.: Global stability of disease-free equilibria in a two-group SI model with feedback control. Nonlinear Anal. Modell. Control **20**, 501–508 (2015)
33. Shang, Y.: Optimal control strategies for virus spreading in inhomogeneous epidemic dynamics. Can. Math. Bull. **56**, 621–629 (2013)
34. Skalski, G.T., Gilliam, J.F.: Functional responses with predator interference: viable alternatives to the Holling type II model. Ecology **81**, 3083–3092 (2001)
35. Tripathi, J.P., Jana, D., Tiwari, V.: A Beddington–DeAngelis type one-predator two-prey competitive system with help. Nonlinear Dyn. **94**(1), 553–573 (2018)
36. Tripathi, J.P., Tyagi, S., Abbas, S.: Global analysis of a delayed density dependent predatorprey model with Crowley–Martin functional response. Commun. Nonlinear Sci. Numer. Simul. **30**, 45–69 (2016)
37. Tripathi, J.P., Abbas, S., Thakur, M.: Dynamical analysis of a preypredator model with Beddington–DeAngelis type function response incorporating a prey refuge. Nonlinear Dyn. **80**, 177–196 (2015)
38. Upadhyay, R.K., Agrawal, R.: Dynamical analysis of a preypredator model with Beddington–DeAngelis type function response incorporating a prey refuge. Nonlinear Dyn. **83**, 821–837 (2016)
39. Volterra, V.: Fluctuations in the abundance of a species considered mathematically. Nature **118**, 558–560 (1926)
40. Xu, J., Teng, Z.: Permanence for a nonautonomous discrete single-species system with delays and feedback control. Appl. Math. Lett. **23**, 949–954 (2010)